ISSN 1674-1056
http://cpb.iphy.ac.cn
http://iopscience.iop.org/cpb
中国物理 B
Chinese Physics
中国物理 Chinese Physics B

Magnetocaloric effect in the layered organic-inorganic hybrid $(CH_3NH_3)_2CuCl_4$

Yinina Ma(马怡妮娜), Kun Zhai(翟昆), Liqin Yan(闫丽琴), Yisheng Chai(柴一晟), Dashan Shang(尚大山), Young Sun(孙阳)
Citation: Chin. Phys. B . 2018, 27(2): 027501. **doi:** 10.1088/1674-1056/27/2/027501

Journal homepage: http://cpb.iphy.ac.cn; http://iopscience.iop.org/cpb

What follows is a list of articles you may be interested in

Influences of La and Ce doping on giant magnetocaloric effect of EuTiO

Zhao-Jun Mo(莫兆军), Qi-Lei Sun(孙启磊), Jun Shen(沈俊), Mo Yang(杨墨), Yu-Jin Li(黎玉进), Lan Li(李岚), Guo-Dong Liu(刘国栋), Cheng-Chun Tang(唐成春), Fan-Bin Meng(孟凡斌)
Chin. Phys. B . 2018, 27(1): 017501. **doi:** 10.1088/1674-1056/27/1/017501

Observation of giant magnetocaloric effect under low magnetic fields in $EuTi_{1-x}Co_xO_3$

Qi-Lei Sun(孙启磊), Zhao-Jun Mo(莫兆军), Jun Shen(沈俊), Yu-Jin Li(黎玉进), Lan Li(李兰), Jun-Kai Zhang(张君凯), Guo-Dong Liu(刘国栋), Cheng-Chun Tang(唐成春), Fan-Bin Meng(孟凡斌)
Chin. Phys. B . 2017, 26(11): 117501. **doi:** 10.1088/1674-1056/26/11/117501

Influence of Ni/Mn ratio on magnetostructural transformation and magnetocaloric effect in $Ni_{48-x}Co_2Mn_{38+x}Sn_{12}$ (x = 0, 1.0, 1.5, 2.0, and 2.5) ferromagnetic shape memory alloys

Ishfaq Ahmad Shah, Najam ul Hassan, Abdur Rauf, Jun Liu(刘俊), Yuanyuan Gong(龚元元), Guizhou Xu(徐桂舟), Feng Xu(徐锋)
Chin. Phys. B . 2017, 26(9): 097501. **doi:** 10.1088/1674-1056/26/9/097501

Effects of Pr substitution on the hydrogenating process and magnetocaloric properties of $La_{1-x}Pr_xFe_{11.4}Si_{1.6}H_y$ hydrides

Lei Xu(许磊), Jin-Liang Zhao(赵金良), Jing-Jie Yang(杨静洁), Hong-Guo Zhang(张红国), Dan-Min Liu(刘丹敏), Ming Yue(岳明), Yi-Jian Jang(蒋毅坚)
Chin. Phys. B . 2017, 26(6): 067502. **doi:** 10.1088/1674-1056/26/6/067502

Magnetic properties and magnetocaloric effect of the Cr-based spinel sulfides $Co_{1-x}Cu_xCr_2S_4$

Xiao-Chao Zheng(郑小超), Xi-Yang Li(李西阳), Lun-Hua He(何伦华), Shao-Ying Zhang(张绍英), Ming-Hua Tang(唐明华), Fang-Wei Wang(王芳卫)
Chin. Phys. B . 2017, 26(3): 037502. **doi:** 10.1088/1674-1056/26/3/037502

Magnetocaloric effect in the layered organic–inorganic hybrid $(CH_3NH_3)_2CuCl_4$*

Yinina Ma(马怡妮娜)[1,2], Kun Zhai(翟昆)[1], Liqin Yan(闫丽琴)[1,†], Yisheng Chai(柴一晟)[1], Dashan Shang(尚大山)[1], and Young Sun(孙阳)[1,2,‡]

[1] *State Key Laboratory of Magnetism and Beijing National Laboratory for Condensed Matter Physics, Institute of Physics, Chinese Academy of Sciences, Beijing* 100190, *China*

[2] *School of Physical Sciences, University of Chinese Academy of Sciences, Beijing* 100190, *China*

(Received 31 October 2017; revised manuscript received 5 December 2017; published online 5 January 2018)

We present a study of magnetocaloric effect of the quasi-two-dimensional (2D) ferromagnet $(CH_3NH_3)_2CuCl_4$ in *ab* plane (easy-plane). From the measurements of magnetic field dependence of magnetization at various temperatures, we have discovered a large magnetic entropy change associated with the ferromagnetic–paramagnetic transition. The heat capacity measurements reveal an abnormal adiabatic change below the Curie temperature $T_c \sim 8.9$ K, which is caused by the nature of quasi-2D layered crystal structure. These results suggest that perovskite organic–inorganic hybrids with a layered structure are suitable candidates as working substances in magnetic refrigeration technology.

Keywords: magnetocaloric effect, organic–inorganic hybrid, $(CH_3NH_3)_2CuCl_4$

PACS: 75.30.sg, 75.50.–y, 81.07.Pr **DOI:** 10.1088/1674-1056/27/2/027501

1. Introduction

The magnetocaloric effect (MCE) is the reversible entropy or temperature change of a magnetic material upon the change of external magnetic field.[1–4] Most of the focus is on achieving high performance with giant magnetic cooling power on rigid inorganic materials. To realize the commercial magnetic refrigerators, vast improvements have been gone through in the search for new magnetic materials in terms of large MCE and relative cooling capacity. A giant MCE has been exhibited in the rigid inorganic materials with three-dimensional (3D) crystal structure such as pseudobinary alloys containing rare earth $Gd_5(Si_2Ge_2)$, $La(Fe_xSi_{1-x})_{13}$, perovskite oxides, sulfide spinels, hexaferrites, etc.[5–12]

During recent decades, the versatility of the organic–inorganic hybrid materials has led to a huge expansion of the organic electronics.[13–21] In particular, the organic–inorganic hybrid halide perovskite materials have attracted intense attention due to the extraordinary photonic and electronic properties.[15–18] However, their potential of caloric effect originating from the ferroelectricity or magnetism has never been noticed, such as $(CH_3NH_3)PbI_3$,[16–18] $(C_nH_{2n+1}NH_3)_2MCl_4$ (M = Mn, Fe, Cu; $n = 1, 2, 3, \ldots$),[19–21] etc. To reveal the multifunctional performance of organic–inorganic hybrid materials and realize their large-scale application eventually, in this paper, the fundamental study on MCE in a prototype organic–inorganic hybrid with two-dimensional (2D) or quasi-2D structure is presented in $(CH_3NH_3)_2CuCl_4$ (MA_2CuCl_4).

The compound MA_2CuCl_4 crystallizes in the layered perovskite structure, consisting of staggered layers of corner-sharing $CuCl_6$ octahedra interleaved by alkylammonium cations $(CH_3NH_3)^+$, as illustrated in Fig. 1(a). It has been proved to be a 2D Heisenberg planar ferromagnet.[22–24] The magnetism comes from Cu ions with an *ab* plane ferromagnetic interaction between the magnetic ions.[22] A very weak ferromagnetic coupling between the layers drives the system to a 3D long-range order at $T_c \sim 8.9$ K.[23] The earlier magnetic studies in this system centered mainly in the behavior of the magnetic susceptibility[23,24] and ferromagnetic resonance (FMR) studies.[25,26] The objective of this paper is to report the studies of the magnetic entropy change with temperature and *ab* plane magnetic field. In addition, we measured the heat capacity under various *ab* plane magnetic fields to calculate the adiabatic temperature change. Eventually, a large magnetic entropy change near T_c is obtained. An abnormal adiabatic temperature change below T_c is also observed.

2. Experiments

Single crystals of MA_2CuCl_4 are naturally grown layer-by-layer along [001] direction by a solvothermal condition method. Yellow plate single crystals with a maximum size of 5 mm×5 mm×0.35 mm are obtained. Powder x-ray diffraction patterns with CuKα radiation revealed the single phase monoclinic perovskite structure with $P2_1/a$, which is in agreement with literature.[27] The magnetization measure-

*Project supported by the National Natural Science Foundation of China (Grant Nos. 51371193 and 11534015), the Youth Innovation Promotion of the Chinese Academy of Sciences (Grant No. 2013004), and the Science Fund from the Chinese Academy of Sciences (Grant Nos. XDB07030200 and KJZD-EW-M05).

†Corresponding author. E-mail: lqyan@iphy.ac.cn

‡Corresponding author. E-mail: youngsun@iphy.ac.cn

© 2018 Chinese Physical Society and IOP Publishing Ltd

ments were performed with a superconducting quantum interference device magnetometer (Quantum Design MPMS) with the magnetic field (B) applied parallel to the metal-halogen layers. The heat capacity was measured under the applied B of 0, 2, and 5 T using a physical property measurement system (Quantum Design).

3. Results and discussion

Figure 1(b) shows the temperature dependence of magnetization under various magnetic fields. The Curie temperature T_c, which is defined as the inflection point in M–T curve at 5 Oe (1 Oe = 79.5775 A·m^{-1}), is 8.9 K, which is consistent with the published data.[23,28] The zero field cooling (ZFC) and field cooling (FC) curves are superposed with each other at 5 Oe and 10 Oe, suggesting a typical ferromagnetic characteristic in ab plane of MA_2CuCl_4. We can also see the Curie temperature and magnetization increase significantly with the increasing magnetic field, implying a potential of large magnetic entropy change.

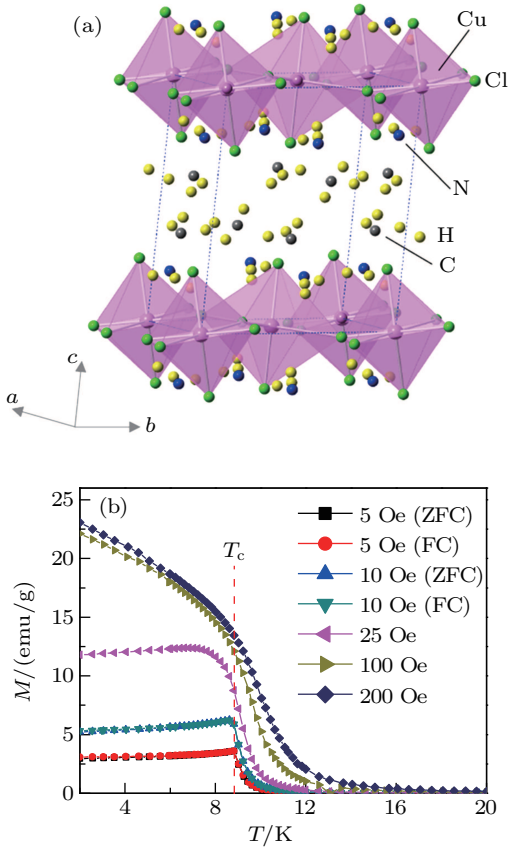


Fig. 1. (color online) (a) The crystal structure of the compound MA_2CuCl_4. (b) The temperature dependences of magnetization for MA_2CuCl_4 in zero-field-cooling (ZFC) at applied magnetic fields of 5, 10, 25, 100, 200 Oe and field-cooling (FC) at magnetic fields of 5, 10 Oe. The red dashed line indicates the Curie temperature T_c determined by the inflection point of low-field M–T curve.

Isothermal magnetization curves were recorded in the temperature range of 5 K–30 K in the magnetic field up to 5 T [Fig. 2(a)]. The temperature step of 1 K is chosen for 5 K–30 K. The sweep rate of field is 40 Oe/s to ensure that M–B curves are recorded in an isothermal process. Figure 2(b) shows Arrott plots of magnetization in which neither the inflection point nor the negative slope is observed above T_c, suggesting the occurrence of a second-order magnetic transition in MA_2CuCl_4.

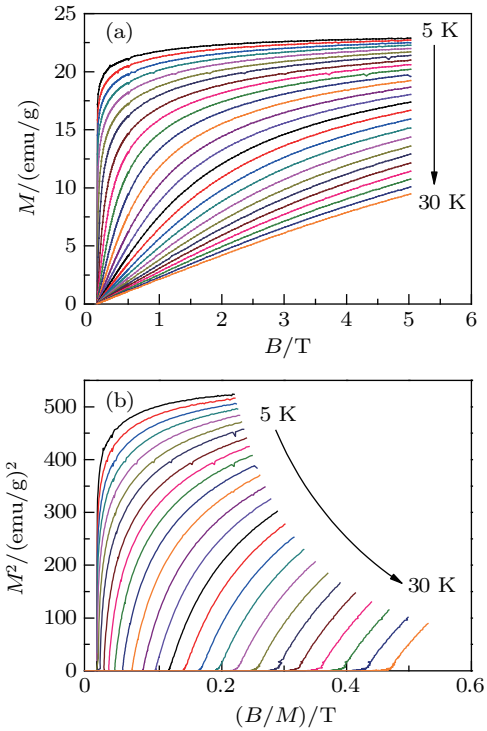


Fig. 2. (color online) (a) Magnetization as a function of applied field of MA_2CuCl_4 measured at 5 K–30 K. (b) The Arrott plots of MA_2CuCl_4.

From the thermodynamical theory, the entropy change generated by the variation of the magnetic field from 0 to H_{max} is given by

$$\Delta S_H = \int_0^{H_{max}} \left(\frac{\partial S}{\partial H}\right)_T \mathrm{d}H, \tag{1}$$

with Maxwell's relation:

$$\left(\frac{\partial M}{\partial T}\right)_H = \left(\frac{\partial S}{\partial H}\right)_T, \tag{2}$$

one obtains the following expression:

$$\Delta S_H = \int_0^{H_{max}} \left(\frac{\partial M}{\partial T}\right)_T \mathrm{d}H. \tag{3}$$

In order to evaluate the entropy change ΔS_H, some methods of numerical approximation to the integral in Eq. (3) are needed. One method is to use isothermal magnetization measurements. In the case of magnetization measurements at small discrete field and temperature intervals, ΔS_H can be approximated from Eq. (3) by

$$|\Delta S_H| = \sum_i \frac{M_i - M_{i+1}}{T_{i+1} - T_i} \Delta H_i, \tag{4}$$

where M_i and M_{i+1} are the experimental values of the magnetization at T_i and T_{i+1}, respectively, under an applied magnetic field H_i. For our sample, the typical sample geometry is

$w = 5$ mm, $h = 3$ mm, and $t = 0.3$ mm and the magnetic field B is applied along the w direction. The demagnetization factor can be roughly calculated to be $N_w \approx 2t/\pi w = 0.038$, which is small enough that we can use B/μ_0 to estimate H.

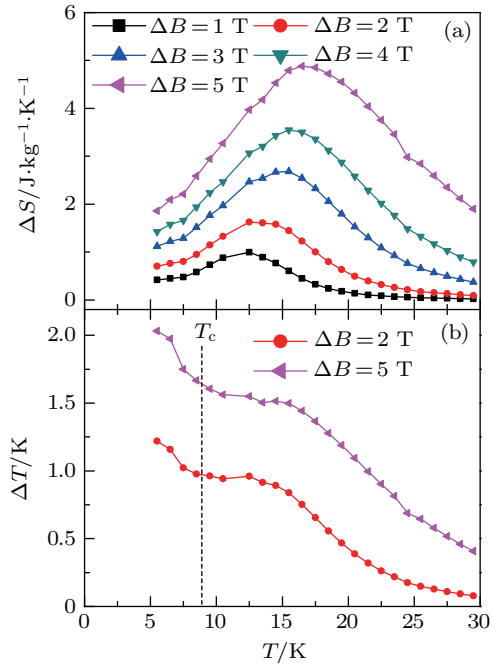


Fig. 3. (color online) (a) Entropy changes in MA_2CuCl_4 extracted from magnetization measurements with the magnetic field changes from 0 to 1, 2, 3, 4, and 5 T. (b) Temperature dependence of adiabatic temperature rise ΔT_{ad} in MA_2CuCl_4 induced by a magnetic field change of 2 T and 5 T.

The entropy changes associated with magnetic field variations have been calculated with Eq. (4). In Fig. 3(a), we plot the magnetic entropy change as a function of temperature for MA_2CuCl_4. As expected from Eq. (3), the peak of magnetic entropy change of MA_2CuCl_4 is at the Curie temperature where the variation of magnetization with the maximum entropy change ΔS_H is 1.72 J/kg·K and 4.98 J/kg·K for the field changes of 2 T and 5 T, respectively. The temperature showing the maximum ΔS_H under $B = 1$ T is 12.5 K, which is higher than the $T_c = 8.9$ K extracted from the magnetization data at low field (5 Oe), shifts to 17 K under $B = 5$ T. Moreover, the ΔS_H spans in a wide temperature range, and the full width of half maximum T approaches to 5 K and 18 K for the magnetic field changes from 0 T to 2 T and to 5 T, respectively. Consequently, relative cooling power (RCP),[29] evaluated by $\mathrm{RCP} = |\Delta S_{H\,\max}| \times \delta T$, reaches 8.6 J/kg and 90 J/kg, respectively. According to thermodynamics, the adiabatic temperature change at an arbitrary temperature T_0 can be expressed as

$$\Delta T \cong -\Delta S_H(T_0, H)\frac{T_0}{C_p(T_0, H)}, \tag{5}$$

where C_p is the specific heat. We further performed the measurements of the heat capacity in the fields of $B = 0$, 2, and 5 T, shown in Fig. 4(a). A thermal anomaly with an inflection slope in zero field corresponding to the magnetic transition is observed, as shown in Fig. 4(b). A broadened discrepancy appears between zero field and 2-T magnetic field above T_c and rounds off in the field of 5 T, indicating a second-order phase transition [see Fig. 4(a)]. If no magnetic transition has taken place at low temperature in MA_2CuCl_4, the low temperature heat capacity would change with decreasing temperature in the same way as that at higher temperature heat capacity (paramagnetic phase), as shown by the extrapolation line in Fig. 4(b). To further confirm the effect of magnetic transition on heat capacity, the relation of C_p/T^3 versus T is plotted, as shown in the inset of Fig. 4(b). A cusp near T_c is clearly observed as indicated by the dashed line, implying the existence of a spin–lattice coupling in the magnetic transition process. Applying a magnetic field can suppress the specific heat below 18 K, which is in accordance with the exchange interaction temperature of nearly isolated quadratic ferromagnetic layers (*ab* plane) from paramagnetic state.

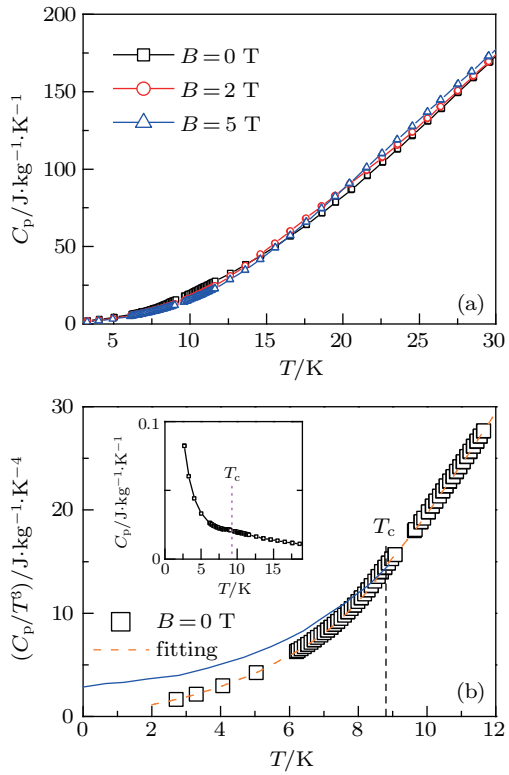


Fig. 4. (color online) (a) Heat capacity of MA_2CuCl_4 measured under the fields of $B = 0$, 2, and 5 T. (b) Heat capacity in zero field and its fitting line (orange color) by the power formula (7) in a range of 2 K–12 K and the extrapolation (blue color) below T_c. The inset shows the temperature dependence of C_p/T^3, the magenta dashed line is the T_c where a kink can be observed.

Based on Eq. (5), the adiabatic temperature rise (ΔT_{ad}) is calculated and presented in Fig. 3(b). The maximum ΔT_{ad} are about 1.3 K and 2.2 K for magnetic field changes of 2 T and 5 T, respectively. We can see the ΔT_{ad} below T_c increases with lowered temperature, indicating the existence of low dimensional heat capacity for MA_2CuCl_4 due to its layered structure. The C_p contribution in zero field is analyzed from crystal

lattice and magnon by using the power law

$$C_{\rm p} = a \times T^{\alpha} + b \times T^{3/2}, \tag{6}$$

where $C_{\rm p}$ is the specific heat, the first term comes from crystal lattice and the second one originates from the ferromagnetic spin wave, to fit the heat capacity below $T_{\rm c}$. The parameters of $\alpha \approx 1.48$, $a = 0.13$, and $b = 0.53$ are obtained, indicating quasi-2D heat capacity nature and the main contribution of heat capacity is arising from magnetic transition below $T_{\rm c}$ since the value of b is larger than a. Based on Eq. (5), the special layered structure abates the heat capacity at low temperature compared to the traditional 3D materials, resulting in an enhancement of $\Delta T_{\rm ad}$ with the decreasing temperature below $T_{\rm c}$.

The large magnetic entropy change in MA_2CuCl_4 must have originated from the considerable increase of magnetization or $T_{\rm c}$ with magnetic fields. With the observation of a large magnetic entropy change and the increasing $\Delta T_{\rm ad}$ in low temperature, one can conclude that a strong spin-lattice coupling in the magnetic ordering process and quasi-2D crystal structure would lead to magnetic entropy change near $T_{\rm c}$ and favors the MCE effect.

Though the maximum of entropy change is smaller than the most conspicuous magnetocaloric materials, MA_2CuCl_4 single crystalline and its derivatives are easy to be synthesized at room temperature and exhibits layered structure as well as potential multicaloric effect that is beneficial for the application in cryogen technique and alternative stimulus.[20,30,31] Besides, since the Curie temperature of organic–inorganic hybrids is easy to modify by the replacement of organic functional group, a large magnetic entropy change may be tuned from low temperature to near room temperature, which is meritful for operating magnetic refrigeration at various temperatures.[30]

4. Conclusions

In conclusion, MA_2CuCl_4 shows a large MCE with its second-order magnetic transition. The results obtained show a large magnetic entropy change near the ferromagnetic–paramagnetic transition and an increasing adiabatic temperature change below $T_{\rm c}$. The large magnetocaloric effect in MA_2CuCl_4 suggests that organic–inorganic hybrid is a suitable candidate as working substance in magnetic refrigeration technology because of (i) large magnetic entropy change, (ii) soft magnetism and reversible MCE, (iii) wide temperature span of ΔS_H and large RCP, (iv) easy to fabricate and tune the magnetic transition temperature by modifying the organic functional group, and (v) potentially multicaloric effect to enhance the MCE.

References

[1] Warburg E Magnetische untersuchungen 1881 *Ann. Phys. Chem.* **13** 141
[2] Gschneidner K A Jr, Pecharsky V K and Tsokol A O 2005 *Rep. Prog. Phys.* **68** 1479
[3] Shen B G, Sun J R, Hu F X, Zhang H V and Cheng Z H 2009 *Adv. Mater.* **21** 4545
[4] Sun Y, Xu X and Zhang Y 2000 *J. Magn. Magn. Mater.* **219** 183
[5] Pecharsky V K and Gschneidner K A Jr 1997 *Phys. Rev. Lett.* **78** 4494
[6] Fujita A, Fujieda S, Hasegawa Y and Fukamichi K 2003 *Phys. Rev. B* **67** 104416
[7] Tegus O, Brück E, Buschow K H J and de Boer F R 2002 *Nature* **415** 150
[8] Yan L Q, Shen J, Li Y X, Wang F W, Jiang Z W, Hu F X, Sun J R and Shen B G 2007 *Appl. Phys. Lett.* **90** 262502
[9] Yan L Q, Chun S H, Sun Y, Shin K W, Jeon B G, Shen S P and Kim K H 2013 *J. Phys.: Condens. Matter* **25** 256006
[10] Huang R, Cao S, Ren W, Zhan S, Kang B and Zhang J 2013 *Appl. Phys. Lett.* **103** 162412
[11] Cao Y, Xiang M, Zhao W, Wang G, Feng Z, Kang B, Stroppa A, Zhang J, Ren W and Cao S 2016 *J. Appl. Phys.* **119** 063904
[12] Fang Y, Yang Y, Liu X, Kang J, Hao L, Chen X, Xie L, Sun G, Chandragiri V, Wang C W, Cao Y, Chen F, Liu Y, Chen D, Cao S, Lin C, Ren W and Zhang J 2016 *Sci. Rep.* **6** 33448
[13] Chen Q Y, Yang H, Huang P R, Ma T, Cao C and He Y 2016 *Chin. Phys. B* **25** 027104
[14] Boix P P, Nonomura K, Mathews N and Mhaisalkar S G 2014 *Mater. Today* **17** 16
[15] Yuan Y, Xu R, Xu H T, Hong F, Xu F and Wang L J 2015 *Chin. Phys. B* **24** 116302
[16] Dong Q, Fang Y, Shao Y, Mulligan P and Qiu J 2015 *Science* **347** 967
[17] Kutes Y, Ye L, Zhou Y, Pang S, Huey B D and Padture N P 2014 *J. Phys. Chem. Lett.* **5** 3335
[18] Huang B, Sun L Y, Wang S S, Zhang J Y, Ji C M, Luo J H, Zhang W X and Chen X M 2017 *Chem. Commun.* **53** 5764
[19] Han J, Nishihara S, Inoue K and Kurmoo M 2015 *Inorg. Chem.* **54** 2866
[20] Caretta A, Miranti R, Havenith R W A, Rampi E, Donker M C, Blake G R, Montagnese M, Polyakov A O, Broer R, Palstra T T M and van Loosdrecht P H M 2014 *Phys. Rev. B* **89** 024301
[21] Lappas A, Zorko A, Wortham E, Das R N, Giannelis E P, Cevc P and Arčon D 2005 *Chem. Mater.* **17** 1199
[22] Becerra C C and Paduan A 2003 *J. Magn. Magn. Mater.* **267** 244
[23] De Jongh L J 1976 *Physica B* **82** 247
[24] Dupas A and Renard J P 1975 *Phys. Lett. A* **53** 141
[25] Demokritov S O, Kreines N M, Kudinov V I and Petrov S V 1989 *Sov. Phys. JETP* **68** 1277
[26] Demokritov S O, Kreines N M, Kudinov V I and Petrov S V 1990 *J. Magn. Magn. Mater.* **90–91** 305
[27] Zolfaghari P, De Wijs G A and De Groot R A 2013 *J. Phys.: Condens. Matter* **25** 295502
[28] Becerra C C, Paduan A 2003 *Solid State Commun.* **125** 99
[29] Gschneidner K A Jr and Pecharsky V K 2000 *Ann. Rev. Mater. Sci.* **30** 387
[30] Kundys B, Lappas A, Viret M, Kapustianyk V, Rudyk V, Semak S, Simon Ch and Bakaimi I 2010 *Phys. Rev. B* **81** 224434
[31] Caretta A, Donker M C, Polyakov A O, Palstra T T M and van Loosdrecht P H M 2015 *Phys. Rev. B* **91** 020405